Miscibility studies in polymer–diluent blends and segmented block copolymers via high-resolution carbon-13 solid-state nuclear magnetic resonance spectroscopy

Laurence A. Belfiore
Department of Agricultural and Chemical Engineering, Colorado State University, Fort Collins, Colorado 80523, USA
(Received 27 March 1985)

Miscibility in blends and short-segmented block copolymers has been studied at the molecular level with the aid of high-resolution solid-state nuclear magnetic resonance (n.m.r.) spectroscopy. The spectroscopic results are in agreement with those from differential scanning calorimetry (d.s.c.). The blend of poly(methyl methacrylate) and 2,2'-dinitrobiphenyl is completely miscible. This is a consequence of near-neighbour interactions between diluent molecules and the pendant groups of the macromolecular chain. The polyether–polyester block copolymers (duPont's Hytrel copolymers) are incompletely phase-separated. Supporting evidence is derived from the observation of n.m.r. signals due to polyester segments dissolved in the polyether-rich mobile domains. As the overall polyester content of the copolymer is increased, molecular mobility in both the crystalline and amorphous domains becomes more restricted. This conclusion is based upon the effect of composition on the proton spin–lattice relaxation times in the rotating frame of reference. Finally, proton dipolar communication via spin diffusion within the soft segment becomes more efficient as the fraction of uncrystallized polyester segments in the polyether-rich domains increases.

(Keywords: miscibility; polymer–diluent blend; copolymers; n.m.r.; spin diffusion)

INTRODUCTION

Statement of the problem

Multicomponent polymer systems have attracted considerable attention recently because of their potential use as practical engineering materials. The global objective of the work described herein is to facilitate the design of these composite materials with the aid of molecular engineering. The role of miscibility in a multicomponent system has a profound influence on the macroscopic properties of the final product[1]. In this respect, high-resolution carbon-13 solid-state nuclear magnetic resonance (n.m.r.) spectroscopy is chosen as the 'site-specific' tool to probe miscibility at the molecular level. For a variety of multicomponent thermoplastics, the n.m.r. results will lend a molecular interpretation of macroscopic behaviour observed in traditional engineering experiments.

Multicomponent polymers

The solid-state morphology of blends and copolymers has been the subject of extensive research[2–6]. In general, most polymer–polymer blends are incompatible. This is the consequence of an extremely small entropy of mixing of two or more components that have reasonably high molecular weights[7]. From a practical standpoint, the physical integrity of a composite polymer system is a strong function of its solid-state morphology and the extent of intermolecular interactions between the components. If one of the blend components is a small molecule, then miscibility and intermolecular interactions are ensured. This is the focus of the initial phase of the work described herein. Large molecule–small molecule mixtures find application in various situations where it is advantageous to lower both the glass transition temperature and the modulus of elasticity of the host polymer. This conventional process is known as plasticization[8]. The physical property alterations associated with plasticization are most dramatic in noncrystallizable materials. In other cases, diluent-induced embrittlement via modulus enhancement gives rise to the well known phenomenon of antiplasticization[9]. The distinction between plasticized and antiplasticized polymers can be established by focusing on the extent of intermolecular interactions[10] in each type of physical blend.

Miscibility-related questions in copolymer systems are somewhat more complex to address than are their counterparts in polymer–diluent systems. This is the consequence of the variety of chain microstructures that are possible for a particular comonomer pair. The solid-state morphology and properties of block copolymers have generated considerable interest because of their practical applicability as thermally processible elastomers. Segmented copolymers, of the $(AB)_n$ type, are alternating block copolymers in which the blocks are relatively short and numerous. Most segmented copolymers exhibit at least a two-phase structure, with the sub-T_g (glassy) or semicrystalline 'hard' segment acting both as a reinforcing filler and multifunctional physical crosslink. It is now widely accepted that the unusual properties of these copolymers are directly related to their multiphase microstructure[3]. Furthermore, the microphase separation is typically incomplete because the copolymer segments are relatively short and not monodisperse in molecular weight. This favours the existence of impure

0032-3861/86/010080-11$03.00

microphases. The resulting interfacial region between the domains comprises a mixed phase in which there is a composition gradient extending from one domain to the other[11]. In some cases, the modelling assumption of sharp interdomain boundaries is supported experimentally[12]. Specifically, the thermodynamics of phase separation imposes restrictions on the topology of the copolymer segments in the vicinity of the interface, leading to microdomain formation[13].

For a particular class of polyether–polyester block copolymers (duPont's Hytrel copolymers), the question of microphase impurity and, therefore, mixing of chemically dissimilar segments is an important one to address. Vallance and Cooper[12] have used a modelling approach to address this topic with the aid of experimental results from calorimetry, X-ray diffraction and dielectric spectroscopy. Since the polyester segments are capable of partial crystallization and the polyether segments are completely amorphous[12], one can pose the following question: Are the uncrystallized polyester segments of the Hytrel copolymers well mixed in the polyether-rich amorphous domains, or do they reside in an 'interphase' region on the periphery of the hard segment (polyester) spherulites? The answer to this and other miscibility-related questions will be formulated at the molecular level with the aid of n.m.r. spectroscopy.

Applications of high-resolution solid-state n.m.r.

In this contribution, high-resolution ^{13}C n.m.r. is used to probe the solid-state morphology of (i) a blend of atactic poly(methyl methacrylate) with 2,2′-dinitrobiphenyl, and (ii) a series of well characterized polyether–polyester segmented block copolymers. Miscibility in multicomponent polymer systems has been investigated previously at the macroscopic level with the aid of techniques such as differential scanning calorimetry (d.s.c.), dynamic mechanical testing, etc.[14–19]. However, the heat capacity *versus* temperature curve obtained from d.s.c. is not as sensitive a probe of miscibility as one might obtain from high-resolution ^{13}C n.m.r. The solid-state n.m.r. experiment is designed to examine the strength of the interaction energy between magnetic-dipolar-coupled nuclei, i.e. ^{1}H and ^{13}C, in different molecules or block copolymer segments. This is facilitated by (i) blending a perdeuterated polymer with a proton-containing additive, or (ii) selectively deuterating only one kind of segment in a block copolymer. In this manner, magnetization can be transferred in an energy-conserving cross-polarization process[20,21], via mutual spin–spin flips, from ^{1}H in the protonated species to ^{13}C in the deuterated species. In spite of the relatively large intermolecular or intersegment distances between ^{1}H and ^{13}C dipolar-coupled nuclides compared to intramolecular couplings, cross-polarization (CP) in the rotating frame of reference provides the necessary pathway for the transfer of nuclear magnetization to occur. However, the rate-determining step for the intermolecular or intersegment cross-polarization process is the proximity of dipolar-coupled nuclides[22], which depends stongly on the state of mixing in the nonequilibrium blend or copolymer.

The dynamics of the cross-polarization process[23] provides one with a method of distinguishing rigid vs. mobile domains and proton-rich vs. proton-starved ^{13}C nuclei. Hence, this experiment is a potentially powerful diagnostic probe of the location of uncrystallized polyester segments in the selectively deuterated Hytrel copolymers. Useful information is embedded in the n.m.r. time constants $T_{CH}(SL)$ and $T_{1\rho}(^{1}H)$, which can be extracted from the time evolution of ^{13}C magnetization during a variable cross-polarization contact-time experiment in the rotating frame. In most situations, the ^{1}H–^{13}C cross relaxation time constant under spin-lock conditions, $T_{CH}(SL)$, characterizes the initial build-up of carbon magnetization[24]. The ^{1}H spin–lattice relaxation time constant in the rotating frame, $T_{1\rho}(^{1}H)$, describes decay of the same ^{13}C magnetization at long CP contact times[22]. This behaviour is observed in a variable CP contact-time experiment when $T_{1\rho}(^{1}H) \gg T_{CH}(SL)$.[23] However, when these time constants are of the same order of magnitude, the time evolution of rare S-spin magnetization, i.e. $S = {}^{13}C$, obeys the following equation[22,25]:

$$\frac{S(t)}{S_{max}} = \frac{1}{1-[T_{CH}(SL)/T_{1\rho}(^{1}H)]} \times \left[\exp\left(-\frac{t}{T_{1\rho}(^{1}H)}\right) - \exp\left(-\frac{t}{T_{CH}(SL)}\right)\right] \quad (1)$$

The CP contact-time dependence of ^{13}C magnetization given by equation (1) is observed typically for resonances in the perdeuterated species. In a completely protonated homogeneous material, spin diffusion within the tightly coupled proton nuclear manifold is, in most cases, a very efficient process. Consequently, the $T_{1\rho}(^{1}H)$ time constant obtained from a fit of equation (1) to the CP contact-time data for each ^{13}C resonance reflects an 'average' $T_{1\rho}(^{1}H)$ characteristic of the system. These trends are not observed in the work described below. The fact that $T_{1\rho}(^{1}H)$ is not averaged completely in both the protonated and selectively deuterated copolymers suggests a solid-state morphology that is inhomogeneous. In other words, the proton spin–spin interactions characteristic of a particular microdomain may not be coupled to the proton interactions in a dissimilar microdomain, especially if there is a dramatic difference in the local segmental mobility of each domain.

EXPERIMENTAL

Nuclear magnetic resonance

Proton-enhanced ^{13}C n.m.r. spectra of copolymers and blends in the solid state were obtained on a Nicolet NT-150 spectrometer at the NSF-supported Regional NMR Center, Colorado State University, Fort Collins, Colorado. The carbon frequency was 37.735 MHz and magic-angle spinning was performed at 2.5–3.5 kHz. The spectrometer incorporates a home-built cross-polarization/magic-angle spinning (CP/MAS) unit, including the probe. The spinner system is a modified version of Wind's[26], with a sample volume of 0.3 cm^3. A proton 90° pulse width of 5 μs was employed, corresponding to an r.f. field strength of 50 kHz. The r.f. field was maintained at 50 kHz during cross-polarization and subsequent high-power ^{1}H decoupling. The ^{13}C free induction decay (FID) was accumulated in a 2 K time-domain window using quadrature detection. Prior to Fourier transformation, the FID was zero-filled to 4 K. The spectral width encompassed a ± 10 kHz frequency range and 5–20 Hz of line broadening was employed. Following Stejskal and Schaefer[27], spin-temperature alternation in the rotating frame was used to suppress the

build-up of artifacts which may occur in proton-enhanced spectra. The sample temperature was maintained at $15 \pm 2°C$ by passing the spinner air through a copper cooling coil immersed in an ice bath.

Differential scanning calorimetry

Glass transition temperatures were measured using a Perkin–Elmer DSC-2B under a nitrogen purge. Approximately 15 mg samples were quenched from the molten state and subsequently scanned at a heating rate of 20 K min^{-1}. T_g was calculated at the midpoint of the heat capacity difference between the liquid and glassy states. In the vicinity of T_g, no heat capacity overshoot was observed in the thermograms due to enthalpic relaxation[28].

Polymer–diluent blend

Perdeuterated poly(methyl methacrylate), d_8-PMMA, was obtained through the courtesy of E. I. duPont de Nemours and Company in Wilmington, Delaware. In order to compare the high-resolution solid-state n.m.r. spectra of protonated and deuterated PMMA, completely hydrogenous atactic PMMA having a molecular weight of 9.3×10^4 (secondary standard) was purchased from Scientific Polymer Products. The 200 MHz ^1H solution n.m.r. spectrum of the deuterated polymer was examined at a concentration of 25 wt% in CD_2Cl_2. By comparison with the previously published ^1H spectra of isotactic and syndiotactic PMMA[29], it was concluded that d_8-PMMA contains a small proportion of protons and that the stereochemistry is predominantly atactic. The percentage deuteration of d_8-PMMA was estimated to be 99.4% from an analysis of the C–H absorption mode at wavenumber 2995 cm^{-1} using a Nicolet MX-1 *FT*i.r. spectrometer. The glass transition temperature (T_g) of d_8-PMMA was found to be 118°C. This is somewhat higher than the accepted T_g of protonated atactic PMMA[30]. However, O'Reilly[31] has mentioned that the effect of deuteration is to increase T_g by about 10°C relative to that of the hydrogenous polymer only in the atactic or stereoirregular case. The low-molecular-weight additive, 2,2'-dinitrobiphenyl (DNB), was purchased from Aldrich Chemicals as a crystalline solid. After heating DNB above the melting point ($T_m = 125°C$) and subsequently quenching it to −100°C, the T_g was found to be −24°C. The 70/30 blend of d_8-PMMA and DNB was prepared by dissolution of the components in dichloromethane and subsequent solvent evaporation. A detailed description of polymer–diluent blend preparation is given elsewhere[32]. Only one T_g was observed for the blend at 55°C while scanning between the temperature limits of −33° and 217°C. Furthermore, no melting transition was observed for DNB in its polymer-mixed state. This suggests that the perdeuterated polymer is compatible with the low-molecular-weight additive on a macroscopic scale. However, the glass transition region of d_8-PMMA is broadened slightly in the presence of the diluent. This suggests a distribution of intermolecular interaction sites in which all segments of the macromolecular chains do not experience the same near-neighbour interactions with DNB.

Segmented block copolymers

The polyether–polyester segmented block copolymers were also supplied by E. I. duPont de Nemours and Company. The chemical structure, average block lengths and overall polyester weight fraction of four well characterized Hytrel copolymers are listed in *Table 1*. The number-average molecular weight of the poly(tetramethylene oxide) (PTMO) soft segment is either 1000 or 2000 and $\bar{M}_n$ of the copolymers is approximately 3.0×10^4. A corresponding series of four well characterized Hytrels, having the same average block lengths as those described in *Table 1*, with completely deuterated poly(tetramethylene terephthalate) segments was also studied. The percentage deuteration of the polyester precursors, dimethyl terephthalate and butanediol, was estimated at 99.3%. In this manner, it was possible to probe the location of uncrystallized polyester segments.

For purposes of comparison, high-molecular-weight homopolymers analogous in structure to the block copolymer segments were also examined by n.m.r. Semicrystalline poly(butylene terephthalate), representative of the polyester segments, was purchased from Aldrich Chemicals and poly(tetrahydrofuran) (PTHF), having a molecular weight of 1.0×10^5 ($\bar{M}_w/\bar{M}_n = 1.04$), was obtained from Polysciences. In the latter case, however, the PTHF homopolymer is semicrystalline whereas the polyether segments of Hytrel are topologically constrained[13] and soft-segment crystallization is suppressed during solidification from the melt[12].

Table 1 Chemical structure and composition of Hytrel block copolymers investigated in this study

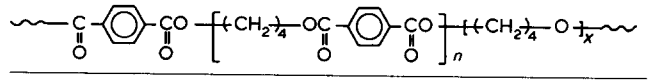

n	$\bar{x}$	Polyether $\bar{M}_n$	Polyester (wt%)
1.6	14	1000	33
4	28	2000	34
4	14	1000	50
9	14	1000	68

RESULTS AND DISCUSSION

Polymer–diluent blend

The high-resolution ^{13}C n.m.r. spectrum of atactic protonated poly(methyl methacrylate) in the solid state is shown in *Figure 1*. Polarization of the various carbons in the repeat unit was obtained via single Hartmann–Hahn contacts[20] with the abundant proton nuclear reservoir in PMMA. The mechanism for cross-polarization transfer is primarily the intramolecular ^1H–^{13}C dipolar

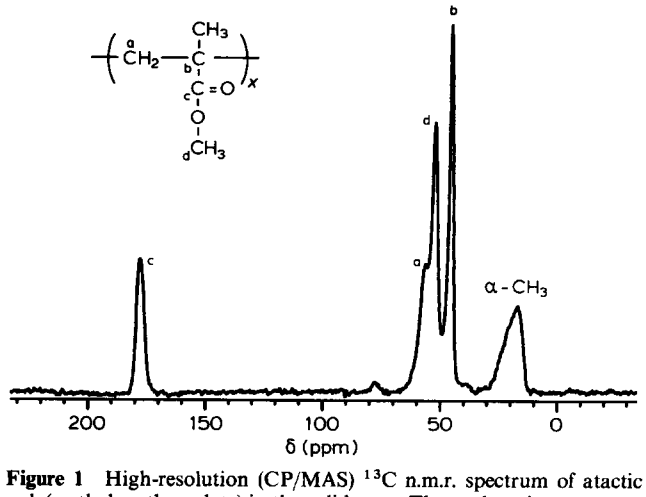

Figure 1 High-resolution (CP/MAS) ^{13}C n.m.r. spectrum of atactic poly(methyl methacrylate) in the solid state. The peak assignments are indicated

coupling. Magnetic-dipolar interactions between ^{1}H and ^{13}C nuclei in neighbouring chains are possible theoretically and may contribute to the cross-polarization ^{13}C n.m.r. spectrum of the PMMA homopolymer. However, this pathway is considered to be of secondary importance relative to the intramolecular interaction, particularly at short cross-polarization thermal mixing times.

Four of the nonequivalent carbons in the repeat unit of PMMA are highly resolved, with the peak assignments[24] given in *Figure 1*. As shown, the backbone methylene carbon exhibits the poorest resolution as a shoulder on the low-field side of the methoxy carbon resonance. This is a consequence of chain stereoirregularity and the variety of rotational states available to the backbone bonds in the glassy homopolymer.

The following 'thought experiments' are helpful to interpret the spectra illustrated in *Figure 2c* and *d*. First, let us replace all eight hydrogen atoms in the PMMA repeat unit with deuterium atoms via an unspecified H–D exchange process. If this process can be taken to completion, then the mechanism by which carbon magnetization is generated in the undiluted homopolymer, cross-polarization via ^{1}H–^{13}C dipolar interactions, is effectively thwarted. The 'proton-enhanced' ^{13}C spectrum of the hypothetical 'completely deuterated' PMMA is shown in *Figure 2c* in the presence of high-power proton irradiation during the data acquisition interval. The fact that one can identify weak signals corresponding to the quaternary and methoxy carbons in the repeat unit suggests that there are residual protons which have survived the H–D exchange process. As stated in the Experimental section, the deuteration efficiency was estimated to be 99.4%. One puzzling observation is the absence of carbonyl intensity in the spectrum of *Figure 2c*. Part of the explanation might stem from the poor signal-to-noise ratio, resulting from time averaging only 750 FIDs at a cross-polarization thermal mixing time of 20 ms.

The second phase of our thought experiment involves the placement of a small molecule, i.e. 2,2′-dinitrobiphenyl, in close proximity to the deuterated PMMA chain. One only requires that (i) the diluent contain some protons, and (ii) the two types of molecules, polymer and diluent, are compatible with each other. The latter requirement is verified macroscopically with the aid of thermal analysis. In performing the solid-state n.m.r. experiment on the two-component mixture, the possibility of generating carbon magnetization in the perdeuterated polymer via ^{1}H–^{13}C dipolar couplings is revived. In this case, however, the cross-polarization pathway is intermolecular in origin. Hence, one has constructed a very sensitive probe of miscibility on a molecule-for-molecule basis.

The proton-enhanced ^{13}C spectrum of the blend of d_8-PMMA and dinitrobiphenyl is shown in *Figure 2d*. This spectrum was also obtained by time averaging 750 FIDs at a cross-polarization contact time of 20 ms. Immediately, upon comparison of *Figures 2c* and *d*, it is evident that the signal-to-noise ratios of the PMMA resonances in the blend are enhanced by at least a factor of 10 relative to those in the undiluted perdeuterated homopolymer. Furthermore, the resonances of d_8-PMMA in the blend spectrum (*Figure 2d*) are very similar in appearance to those of the undiluted protonated homopolymer illustrated in *Figure 1*. These facts suggest that the mixing process affects the local environment of PMMA chain segments to the extent that molecules of dinitrobiphenyl interact with the polymer as nearest neighbours. One arrives at a similar conclusion from a macroscopic viewpoint by measuring glass transition temperatures with a differential scanning calorimeter.

It is advantageous to investigate the dynamics of intermolecular cross-polarization for the blend of d_8-PMMA and dinitrobiphenyl. In this experiment, one follows the evolution of ^{13}C magnetization in both polymer and diluent as a function of the time during which the ^{1}H and ^{13}C nuclear reservoirs are allowed to exchange energy, approach equilibrium (achieve a common spin temperature) and then interact with the lattice. The result is a contact-time curve as shown in *Figure 3*. The time constants $T_{CH}(SL)$ and $T_{1\rho}(^{1}H)$ can be de-

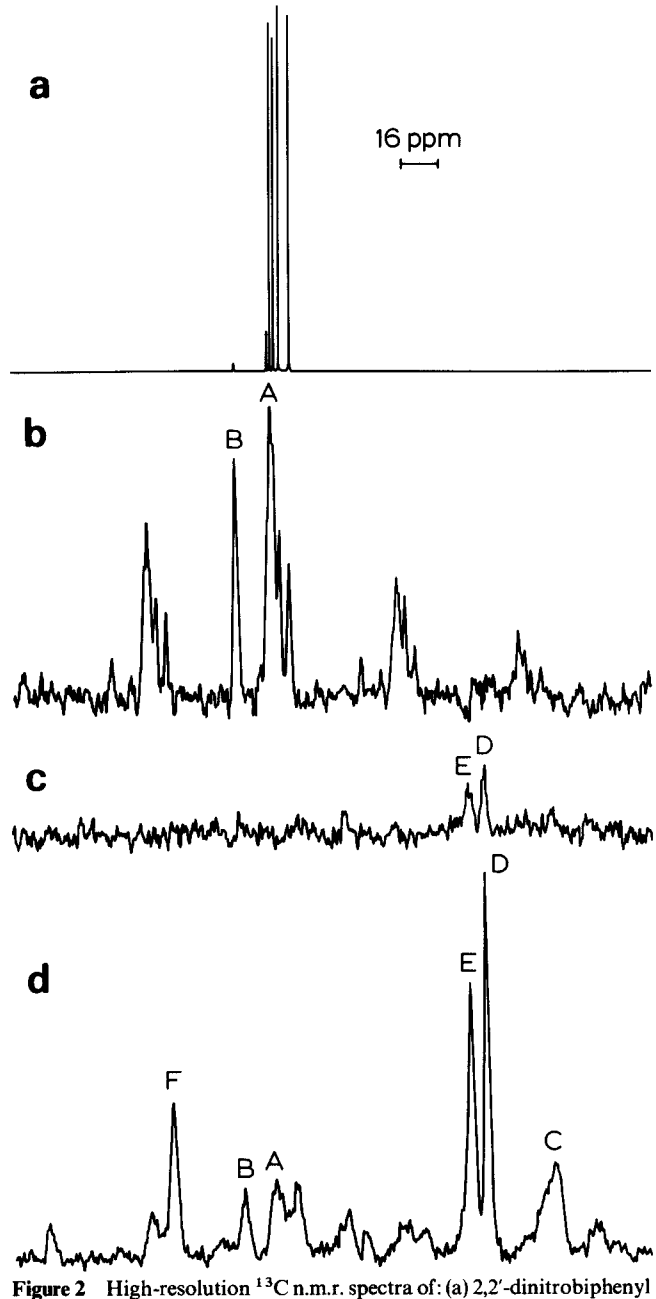

Figure 2 High-resolution ^{13}C n.m.r. spectra of: (a) 2,2′-dinitrobiphenyl (25 wt%) in hexachlorobutadiene (solvent peaks removed) at 110°C; (b) 2,2′-dinitrobiphenyl in the solid state (crystalline) from 750 FIDs at a CP contact time of 6 ms; (c) d_8-PMMA in the solid state (amorphous) from 750 FIDs at a CP contact time of 20 ms; (d) 70/30 blend of d_8-PMMA and DNB in the solid state (amorphous) from 750 FIDs at a CP contact time of 20 ms. The resonances designated by A and B correspond to the diluent; those designated by C, D, E and F are contributions from d_8-PMMA (see *Figure 3*)

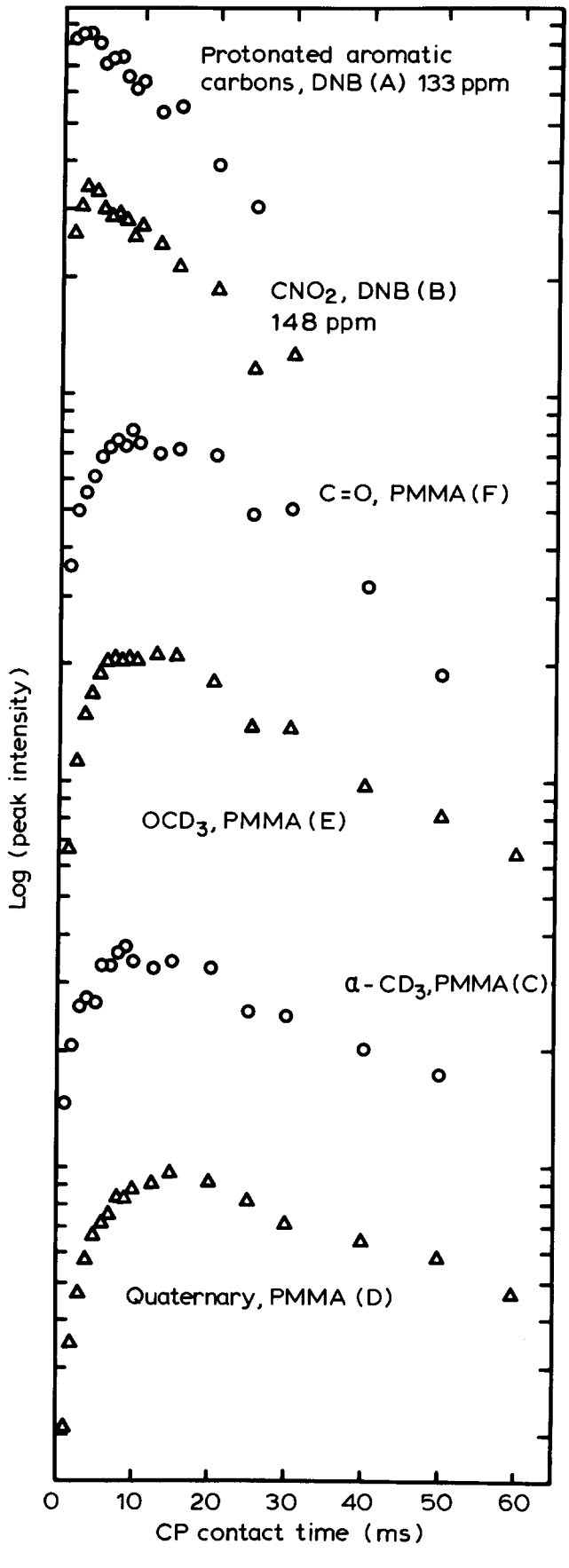

Figure 3 ^{1}H–^{13}C cross-polarization contact-time curves for the ^{13}C resonances of both the diluent and the polymer in a 70/30 blend of d_8-PMMA and dinitrobiphenyl. The vertical scale has been shifted for clarity. The letters in parentheses correspond to the labelled peaks in *Figure 2*

termined at most of the carbon sites in both blend components from a fit of equation (1) to the contact-time data. $T_{CH}(SL)$ is a spin–spin parameter that is very sensitive to the spectral density of near-static ^{1}H–^{13}C dipolar interactions[33], whereas $T_{1\rho}(^{1}H)$ is a spin–lattice parameter predominantly sensitive to the spectral density of homonuclear ^{1}H–^{1}H dipolar modulations at twice the proton radio-frequency field strength in the rotating frame of reference[34]. A relatively short value for $T_{CH}(SL)$ is characteristic of a rigid system with short ^{1}H–^{13}C dipolar distances. In general, either highly mobile or proton-starved ^{13}C nuclei will exhibit relatively long cross-relaxation time constants. More important than the dependence of $T_{1\rho}(^{1}H)$ on motion is the fact that efficient proton spin diffusion due to relatively strong ^{1}H–^{1}H dipolar couplings tends to average $T_{1\rho}(^{1}H)$ to a single value[35]. This average value of $T_{1\rho}(^{1}H)$ is, of course, only observed at carbon locations that are encompassed by the tightly coupled proton spin-diffusion process. In a phase-separated material, for example, interdomain spin diffusion is not very efficient if the local segmental mobility of each domain is considerably different. Hence, one should not expect to observe an average $T_{1\rho}(^{1}H)$ at all carbon sites.

The time evolution of ^{13}C magnetization in the blend of d_8-PMMA and DNB is shown in *Figure 3*. As mentioned above, these data were generated from a variable-contact-time experiment. It is important to focus on two different contact-time regimes in these curves. The short-contact-time regime is primarily governed by the time constant $T_{CH}(SL)$. As expected, $T_{CH}(SL)$ is relatively short for the ^{13}C nuclei of the diluent, dinitrobiphenyl. This is a consequence of the fact that the DNB carbons either have directly bonded protons or they are adjacent to carbons having directly bonded protons. In either case, the carbons are fairly rigid and not proton-starved. In contrast, the carbons in d_8-PMMA are proton-starved. This is reflected by the relatively slow build-up of ^{13}C magnetization in the perdeuterated polymer. Of equal importance is the time dependence of ^{13}C magnetization in the long-contact-time regime. In this case, $T_{1\rho}(^{1}H)$ is the primary governing parameter. A summary of both time constants, $T_{CH}(SL)$ and $T_{1\rho}(^{1}H)$, is given in *Table 2* for the 70/30 blend of d_8-PMMA and DNB. These parameters were obtained from a nonlinear fit of the contact-time data to equation (1) for each ^{13}C resonance that is resolvable in the CP/MAS spectrum of the blend. It is evident that proton spin diffusion is operative within the diluent molecules since $T_{1\rho}(^{1}H)$ is approximately the same when evaluated at either the protonated or nitrogenated aromatic carbon sites. However, the tightly coupled spin-diffusion process within the proton nuclear system of DNB is not efficient enough to average all of the experimentally observed $T_{1\rho}(^{1}H)$ values in d_8-PMMA to a single value. The difference between $T_{1\rho}(^{1}H)$ measured at the carbonyl and quaternary carbons is more than a factor of 2. This is believable if one considers the broad distribution of carbon–proton intermolecular distances that may be involved in the cross-polarization process. This state of mixing is unavoidable for a blend containing only 30% DNB on a weight basis in which not all of the chain segments of d_8-PMMA are adjacent to molecules of DNB.

The $T_{1\rho}(^{1}H)$ data in *Table 2* suggest that the carbonyl carbon in d_8-PMMA shares a local environment with the

Table 2 Parameters governing the time evolution of ^{13}C magnetization in the CP contact-time experiment. The blend is a 70/30 mix of d_8-PMMA and 2,2'-dinitrobiphenyl

	$T_{CH}(SL)^a$ (ms)	$T_{1\rho}(^1H)^a$ (ms)
DNB		
aromatics	0.6	23
CNO_2	1.0	26
d_8-PMMA		
C=O	8.2	20
OCD_3	3.7	37
α-CD_3	4.0	48
quaternary	6.8	50

[a] Time constants $T_{CH}(SL)$ and $T_{1\rho}(^1H)$ were obtained from a nonlinear fit of the data in *Figure 3* to equation (1). Maximum uncertainty is $\pm 22\%$ for $T_{CH}(SL)$ and $\pm 10\%$ for $T_{1\rho}(^1H)$

carbons of DNB in close proximity to the DNB protons. However, this claim is not supported by the $T_{CH}(SL)$ data, which indicates that the build-up of magnetization via intermolecular C–H dipolar couplings is slowest at the carbonyl carbon. This dichotomy is probably the consequence of an extremely complicated intermolecular cross-polarization process. Moreover, it is possible that carbonyl mobility in PMMA modulates the chemical shift anisotropic interaction at the carbonyl nucleus causing efficient relaxation during cross-polarization. This might explain the relatively long $T_{CH}(SL)$ and short $T_{1\rho}(^1H)$ time constants for the carbonyl carbon. Nevertheless, the relatively short $T_{CH}(SL)$ values of 3.7 and 4.0 ms for the methoxy and α-methyl carbons, respectively, of d_8-PMMA are in agreement with a structural model that places these two polymer carbons in a near-neighbour environment with molecules of the protonated additive.

Segmented block copolymers

Before presenting solid-state ^{13}C n.m.r. spectra of the Hytrel copolymers, whose chemical architectures are described in the Experimental section, it is instructive to look first at some high-molecular-weight homopolymers that are analogous in structure to the block copolymer segments.

Protonated homopolymers. The semicrystalline polyester segments of the Hytrel copolymers are essentially oligomers of butylene terephthalate with segment molecular weights ranging from 500 to 2000. The proton-enhanced ^{13}C n.m.r. spectrum of high-molecular-weight semicrystalline poly(butylene terephthalate) (PBT) is shown in *Figure 4*. Also included in *Figure 4* are the peak assignments[36] and the average value of $T_{1\rho}(^1H)$ at 50 kHz. In other words, the fit of equation (1) to the contact-time curve for each of the five resonances of PBT yields a $T_{1\rho}(^1H)$ of 1.6 ms. As discussed above, the observation of an average $T_{1\rho}(^1H)$ at each carbon site is expected if the system is homogeneous and consists of a single phase. However, the semicrystalline nature of PBT suggests the existence of at least a two-phase morphology composed of crystalline and amorphous domains. The underlying reason for the failure of the n.m.r. cross-polarization experiment to distinguish between two coexisting phases in PBT might be due to the fact that carbons in crystalline and amorphous regions are not resolved in the n.m.r. spectrum. Hence, each resonance line in *Figure 4* contains both crystalline and amorphous contributions that overlap extensively. Surprisingly, the long-time regime of each contact-time curve for PBT does not exhibit bi-exponential decay. One would probably predict *a priori* that two different $T_{1\rho}(^1H)$ values are necessary to describe accurately the long-time decay of carbon magnetization in a CP experiment, especially if the magnetization results from a superposition of signals in two different domains. However, the fact that the amorphous domains of PBT are in the glassy state at ambient temperature ($T_g = 50°C$) suggests that interdomain dipolar interactions within the proton nuclear system of PBT might be operative. This coupling between crystalline and rigid amorphous domains might average all of the experimentally observed $T_{1\rho}(^1H)$ values to a single value in the semicrystalline homopolymer.

The amorphous polyether segments of the Hytrel copolymers are poly(tetramethylene ether glycol) with a number-average molecular weight of either 1000 or 2000. As discussed by Vallance and Cooper[12], polyether crystallization is suppressed upon cooling the undiluted polymer melt. This is understood if one follows the series of isothermal events (first- and second-order transitions) that occur upon cooling the Hytrel materials to ambient temperature from the molten state. Initially, one observes crystallization of, at most, 50% of the polyester segments. Depending on the segment length of poly(tetramethylene terephthalate), melting temperatures range from about 200°C to 225°C[12] and crystallization can be expected to occur about 50°C below T_m during the cooling cycle. Next, one observes vitrification of the uncrystallized polyester segments in the temperature range 40°C–50°C. At this point, the covalently bound ends of the polyether segments are anchored by the adjacent polyester segments. This topological constraint prohibits conformational rearrangements of the polyether backbone bonds. Hence, it is virtually impossible for the polyether segments to adopt an all-*trans* conformation, which is necessary for crystallization to occur[37].

Incidentally, the melting temperatures of various molecular weights of poly(tetramethylene ether glycol) range from about 35°C to 49°C[38] and crystallization of a high-molecular-weight analogue has been observed at approximately 10°C upon cooling the undiluted melt[38]. This observation provides further support for a completely amorphous polyether phase at ambient temperature.

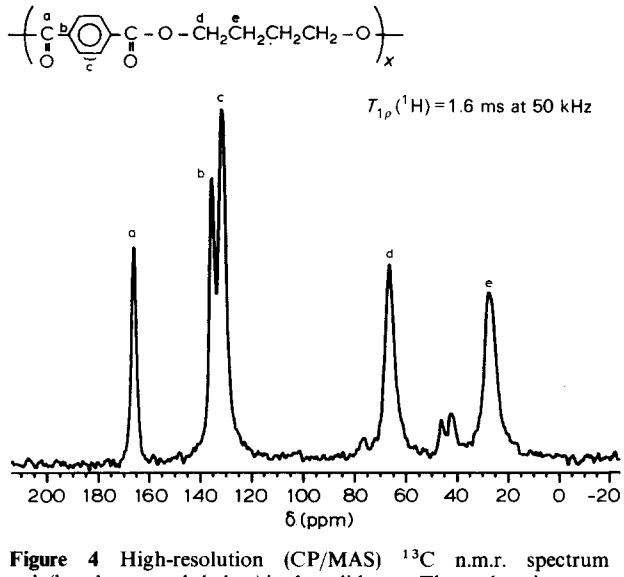

Figure 4 High-resolution (CP/MAS) ^{13}C n.m.r. spectrum of poly(butylene terephthalate) in the solid state. The peak assignments are indicated

A variety of high-resolution ^{13}C n.m.r. spectra of high-molecular-weight semicrystalline poly(tetramethylene oxide) are shown in *Figure 5* together with peak assignments and cross-polarization contact times listed at the left. Contrary to the spectrum of poly(butylene terephthalate) in *Figure 4*, the crystalline and amorphous resonances of both types of methylene carbons in poly(tetramethylene oxide) are resolved and can be observed selectively by using the proper choice of cross-polarization contact time. For example, the top spectrum at 50 μs contact in *Figure 5* reveals primarily carbons in the crystalline regions. The strength of the C–H dipolar couplings within the crystallites is responsible for the relatively short values of T_{CH}(SL) for these carbons and the appearance of a spectrum at such a short CP contact time. On the other hand, the spectrum at 10 ms of CP contact reveals primarily the amorphous carbons. These two resonance lines are quite narrow; a result of extremely mobile amorphous domains in which the glass transition temperature is found in the range $-83°C$ to $-88°C$.[39] In fact, molecular motion in the amorphous domains of poly(tetramethylene oxide) is rapid enough to render a high-resolution spectrum under experimental conditions reserved for liquid-like samples (see the scalar-decoupled spectrum in *Figure 5*, bottom). As expected, carbons in both domains are observed simultaneously at an intermediate contact time of 700 μs (see *Figure 5*). This raises the question of the origin of the chemical shift difference between carbons in crystalline and amorphous domains. For the present example of poly(tetramethylene oxide), the internal methylene carbons are separated by 1 ppm and the external (oxygen-linked) ones are separated by 2 ppm; in both cases, the amorphous resonance is upfield (to the right) in relation to the corresponding crystalline resonance. There are several examples in the literature which report chemical shift differences between carbons in amorphous and crystalline regions of semicrystalline homopolymers. These include polyethylene[40], polyoxymethylene[41], poly(ethylene oxide)[42], 1,4-*trans*-polybutadiene[43] and poly(ethylene terephthalate)[44,45]. Similar examples have been reported for a variety of biological macromolecules, with cellulose being the classic example[46–48].

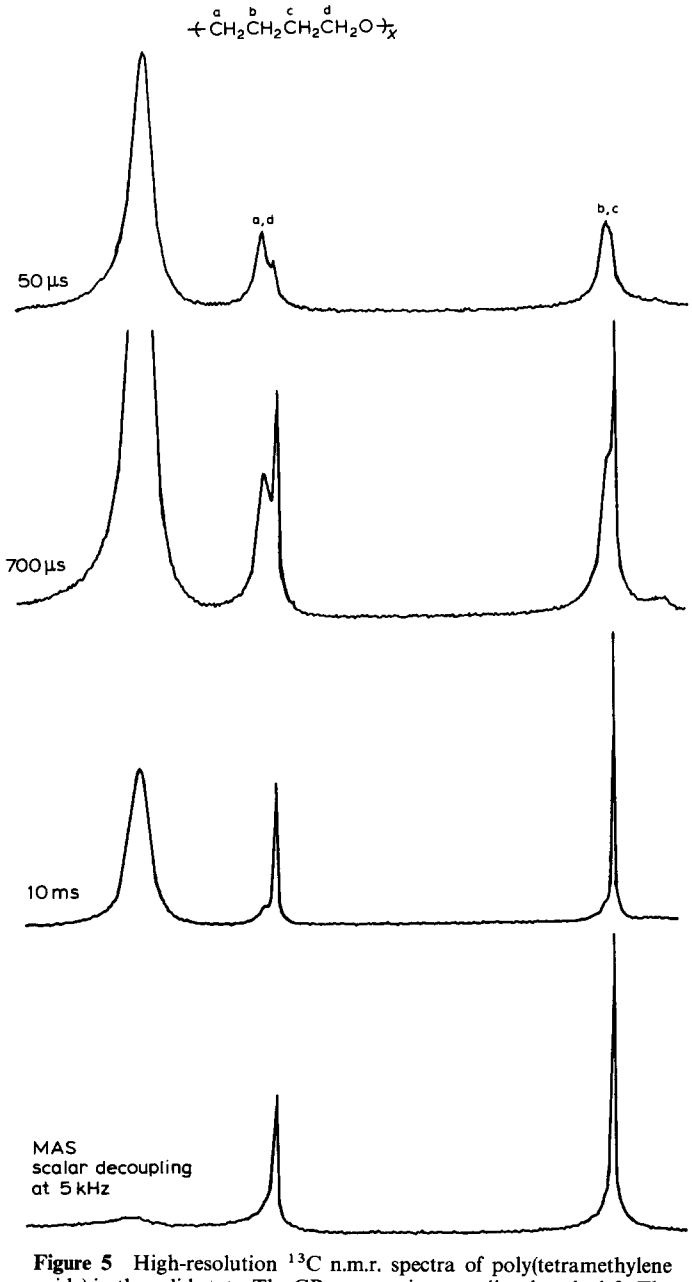

Figure 5 High-resolution ^{13}C n.m.r. spectra of poly(tetramethylene oxide) in the solid state. The CP contact times are listed at the left. The bottom spectrum was obtained under liquid-like conditions in the presence of magic-angle spinning

In all of the examples mentioned above, the chemical shift differences are understood by applying Tonelli's γ-*gauche* method[49]. This is an empirical scheme that relies on results from both wide-angle X-ray diffractometry to quantify the crystalline chain conformation and rotational isomeric state calculations to determine occupational probabilities of backbone bonds in the bulk amorphous state. Using this information, Tonelli[49,50] has shown that carbon atoms separated by three bonds in a *gauche* conformation interact and experience increased chemical shielding. This results in an upfield chemical shift of the γ-*gauche* carbons relative to the same type of carbons in a *trans* arrangement. Therefore, since the crystalline backbone conformation of poly(tetramethylene oxide) is necessarily comprised of only one type of bond-rotational state (all *trans*)[37], the upfield chemical shifts of the amorphous carbons are understood qualitatively with the aid of the γ-*gauche* method. In other words, it is tacitly assumed that the amorphous backbone conformations of poly(tetramethylene oxide) contain some *gauche* rotational states that are foreign to the crystal.

Protonated copolymers. The high-resolution proton-enhanced ^{13}C n.m.r. spectrum of a Hytrel copolymer in the solid state is shown in *Figure 6*. In this example, the molar ratio of dimethyl terephthalate to 1,4-butanediol to poly(tetramethylene ether glycol) is 10/9/1 with a number-average molecular weight of 1000 for the polyether soft segment. As discussed above for the protonated PMMA homopolymer, the generation of carbon magnetization via the cross-polarization process proceeds primarily through intramolecular ^{1}H–^{13}C dipolar interactions within the protonated copolymer chain. Whether or not intersegment polarization transfer is operative in the completely protonated material is a difficult question to address based on the experimental conditions used to obtain the spectrum in *Figure 6*. However, this mechanism is discussed below with the aid of some tailor-made copolymers in which the polyester segments are completely deuterated.

The high-resolution spectrum in *Figure 6*, for which the

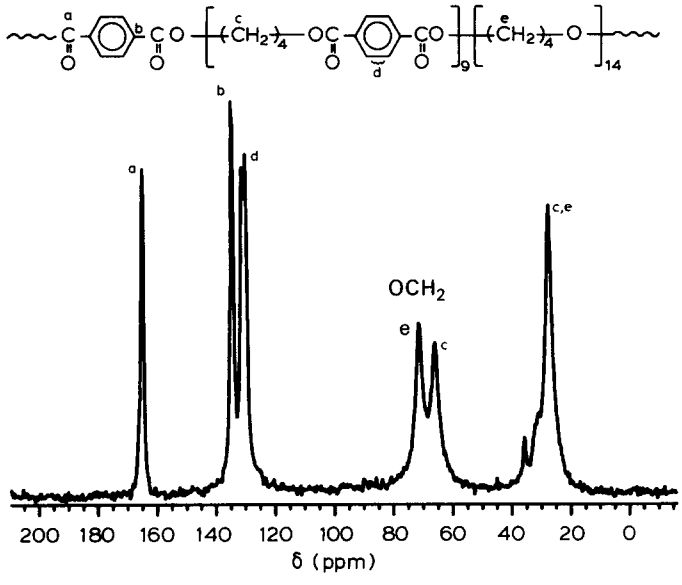

Figure 6 High-resolution (CP/MAS) ^{13}C n.m.r. spectrum of a polyether–polyester segmented block copolymer in the solid state at a CP contact time of 800 μs. The polyester weight fraction is 0.68 and the peak assignments are indicated

polyester weight fraction is approximately 0.68, is nothing more than a superposition of spectra from the polyester and polyether segments whose high-molecular-weight analogues are shown in *Figures 4* and *5*, respectively. Of course, the crystal vs. amorphous splittings of the interior and exterior (downfield) methylene lineshapes of poly(tetramethylene oxide) shown in *Figure 5* are absent in the copolymer spectrum because of the completely amorphous nature of the polyether segments. The peak assignments of Hytrel, as indicated in *Figure 6*, have been reported previously, both in solution[51] and in the solid state[36]. Evidence to support these assignments has been obtained by incorporating a dipolar-dephasing delay in the cross-polarization pulse sequence and monitoring the rapid decay of the protonated carbon resonances (aromatics and oxygen-linked methylenes) that are unique to the polyester hard segments. The lineshapes of the central methylene carbons in both segments significantly overlap each other such that only one resonance line is observed at about 28 ppm. One further point of interest is the splitting of the lineshape in *Figure 6* which contains signals from the four protonated aromatic carbons of the terephthalate unit. This suggests the possibility of, at least, two conformations for the

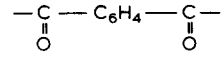

portion of the polyester segment. The observed doublet for the protonated aromatic carbons might be the consequence of two distinct crystalline conformations of the planar terephthalate unit[52] which are essentially static on the n.m.r. timescale[53]. Another possibility which is, most likely, less probable is that one is observing ring carbons in both crystalline and amorphous regions of the copolymer.

Deuterated copolymers. Let us consider again an analogous 'thought experiment', this time involving the Hytrel copolymer discussed above, in which all of the hydrogen atoms in the polyester repeat unit are replaced by deuterium atoms via an H–D exchange process. In this case, the only source of carbon magnetization via ^{1}H–^{13}C cross-polarization is the proton nuclear reservoir of the tetramethylene units within the polyether segments. Hence, either intersegment or intermolecular cross-polarization mechanisms must be operative if one observes carbon signals from the polyester segments in a proton-enhanced ^{13}C n.m.r. spectrum. The viability of these two mechanisms requires that some of the polyester segments must be dissolved in the amorphous domains which contain all of the mobile polyether segments. In other words, in the absence of relatively strong inter-domain carbon–proton dipolar couplings, which is very probable when one of the domains (polyether) is extremely mobile, some type of segmental mixing is required if polyester carbon resonances are observed in a CP spectrum of the selectively deuterated Hytrel copolymers. Such a spectrum is seen in *Figure 7* in which the polyester weight fraction is about 0.68. The peak assignments follow directly from those shown in *Figure 6*. The appearance of four distinct lineshapes corresponding to the carbonyl, nonprotonated aromatic, protonated aromatic, and oxygen-linked methylene carbons of the polyester repeat unit suggests that phase mixing is, indeed, characteristic of the solid-state morphology of the short-segmented block copolymers. This is in agreement with results of differential thermal analysis on the Hytrel copolymers[18], which reveal an increase in the glass transition temperature of the soft segment, above $-88°C$ for pure poly(tetramethylene oxide), with increasing weight fraction of polyester (or, equivalently, increasing hard-segment block length)[54]. In other words, T_g increases as more polyester segments are randomly mixed in the amorphous polyether phase.

However, one might suspect, and rightly, that the origin of ^{13}C magnetization in the deuterated polyester segments is the consequence of an intrasegment cross-polarization mechanism. This is possible if there are residual polyester protons that survive the H–D exchange process. Since an examination of 'completely' deuterated poly(tetramethylene terephthalate) in the absence of the polyether phase was not possible in this study, one cannot discard the intrasegment CP mechanism solely on the

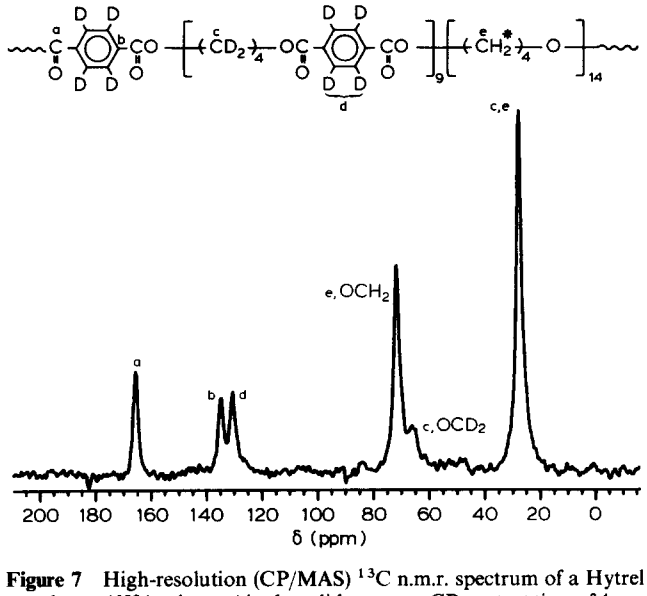

Figure 7 High-resolution (CP/MAS) ^{13}C n.m.r. spectrum of a Hytrel copolymer (68% polyester) in the solid state at a CP contact time of 4 ms. The polyester segments are completely deuterated and the peak assignments are indicated

appearance of the copolymer spectra in *Figures 6* and *7*. In this respect, results of a variable-contact-time study on both the protonated and selectively deuterated copolymers are discussed below to answer the following questions.

(1) What cross-polarization mechanism is primarily responsible for the appearance of polyester carbon resonances in the CP n.m.r. spectra of selectively deuterated Hytrel copolymers?

(2) Are the results of the n.m.r. method consistent with the morphological description of Hytrel, which favours intersegment mixing[12] in the amorphous domains?

Cross-polarization contact-time results. The time evolution of ^{13}C magnetization in both the polyester and polyether segments of a Hytrel copolymer during a contact-time experiment is illustrated in *Figure 8*. The abscissae indicate the duration of cross-polarization thermal mixing between the proton and carbon nuclear spin reservoirs. Data points represented by circles correspond to ^{13}C magnetization in the protonated copolymer. For the Hytrel material (68% polyester, number-average molecular weight of 1000 for the polyether segments) in which the polyester segments are completely deuterated, the contact-time data are depicted by the squares. In all cases shown in *Figure 8*, the logarithmic (vertical) axis has been shifted vertically to facilitate comparison of the data. In other words, the absolute magnitude of the carbon peak heights is unimportant in the rate analysis of the contact-time curves that follows.

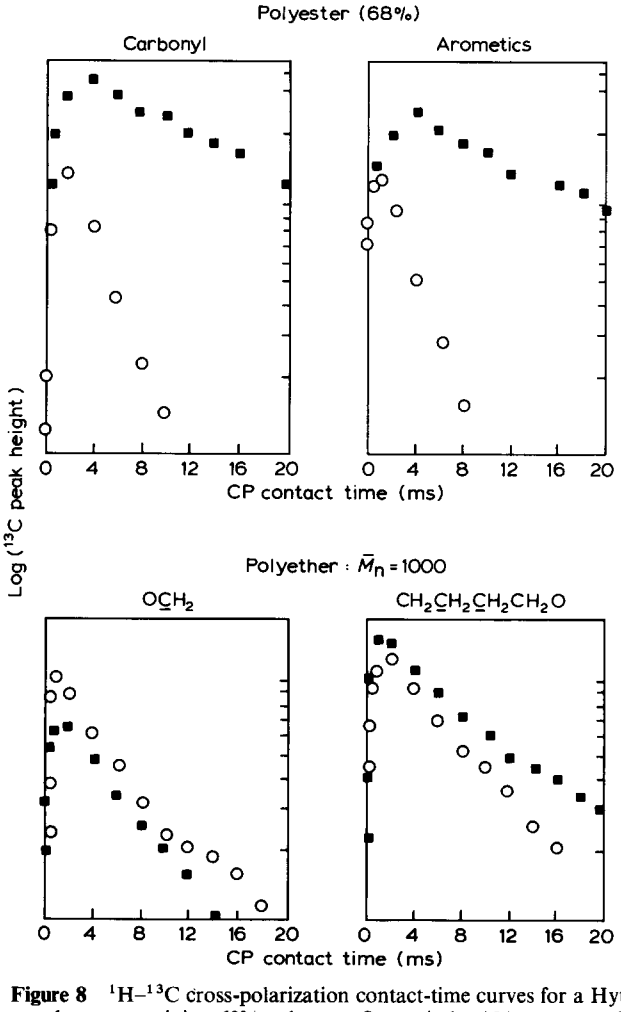

Figure 8 ^{1}H–^{13}C cross-polarization contact-time curves for a Hytrel copolymer containing 68% polyester. Open circles (○) correspond to carbon peak heights in the completely protonated copolymer. Filled squares (■) depict the situation when the polyester segments are completely deuterated

Straightforward observation of the results of the variable-contact-time experiment (*Figure 8*) leads one to the following qualitative interpretation with respect to the predominant mechanism of cross-polarization in the selectively deuterated copolymer.

(1) The long-time decay behaviour of peak heights for both the aromatic and carbonyl polyester carbons is almost identical in the completely protonated Hytrel copolymer (circles in the upper two graphs of *Figure 8*). This suggests that relatively strong proton–proton dipolar interactions are operative within the rigid polyester domains. Hence, the experimentally observed $T_{1\rho}(^{1}H)$ time constants, measured at various carbon sites in the polyester segment, reflect an average relaxation time which characterizes communication between the polyester proton spin system and the lattice.

(2) For the internal and external (oxygen-linked) methylene carbons in the polyether segments, the long-time decay behaviour of the carbon peak heights (indicated by circles in the lower two graphs of *Figure 8*) is markedly slower than relaxation in the polyester segment. This indicates that intersegment and, most likely, interdomain spin diffusion within the proton nuclear system of the copolymer are not capable of averaging $T_{1\rho}(^{1}H)$ to one value in both segments. Instead, one observes a characteristic $T_{1\rho}(^{1}H)$ for the polyether segment which is considerably longer than that for the polyester segment. This behaviour is expected in a phase-separated material in which one of the phases is highly mobile (polyether) and the other phase is quite rigid (polyester).

(3) The cross-polarization contact-time behaviour of the polyether methylene carbons is essentially unaffected when the polyester segments of the copolymer are completely deuterated (data represented by squares in the lower two graphs of *Figure 8*). This result favours an intrasegment cross-polarization mechanism within the polyether domains in which methylene carbon magnetization is derived from directly bound protons. In neither of the two materials investigated are the polyether carbons proton-starved.

(4) Finally, one observes that the time evolution of carbon magnetization in the completely deuterated polyester segments (data represented by squares in the upper two graphs of *Figure 8*) is immensely different from the contact-time curves for the polyester carbons in the protonated copolymer. The relatively slow build-up of carbon magnetization (between 0 and 4 ms) in the deuterated polyester segments suggests that carbon–proton dipolar interactions, which provide the viable cross-polarization pathway, are quite weak. Weak dipolar interaction can arise either from a coupling between highly mobile nuclei or from carbons that are proton-starved. In both cases, the experimental results argue in favour of a cross-polarization mechanism that is either intermolecular or intersegment in origin. This is further supported by the long-time behaviour of the data in *Figure 8*. If an intrasegment CP mechanism due to residual protons is operative within the polyester domains of the selectively deuterated Hytrel copolymer, then one should not observe contact-time curves for the polyester carbons that are so much different in the deuterated material relative to those in the protonated material.

Hence, the answer to our first question can be stated as follows: Carbon magnetization in the selectively deuterated polyester segments of Hytrel, which is shown in the n.m.r. spectrum of *Figure 7*, is the consequence of weak magnetic-dipolar interactions between the polyester carbons and the polyether protons.

Our final goal is to pinpoint the location of the deuterated polyester segments that are responsible for the polyester contribution to the ^{13}C n.m.r. spectrum in *Figure 7*. In this manner, it is shown that n.m.r. can offer its own description of the morphological state of the Hytrel segmented block copolymers. The $T_{1\rho}(^1H)$ time constants at 50 kHz for each of the copolymers described in the Experimental section are given in *Table 3*. These data were obtained from a nonlinear fit of Equation (1) to the cross-polarization contact-time curves for each individual carbon resonance. The only carbon sites for which data are not readily available are the interior methylene carbons of the polyester segment. This is a consequence of their chemical shift overlap with the interior methylene carbon resonance of the polyether segment at 28 ppm in the spectrum. The numbers in parentheses in *Table 3* correspond to the $T_{1\rho}(^1H)$ time constants for the copolymers that have completely deuterated polyester segments.

If one focuses on the $T_{1\rho}(^1H)$ time constants within the protonated polyester segments, it is evident that efficient proton spin diffusion is operative within the polyester domains. Thus, for each copolymer composition, the experimental results yield only an averaged value of $T_{1\rho}(^1H)$ for the polyester segments. Furthermore, the polyester $T_{1\rho}(^1H)$ values decrease continuously from approximately 6.9 ms to 3.4 ms as the polyester content of the copolymer increases. This trend in polyester 'average' $T_{1\rho}(^1H)$ vs. copolymer composition is not inconsistent with the average value of 1.6 ms quoted above for poly(butylene terephthalate) in the limit of pure polyester. Vallance and Cooper[12] have presented calorimetric data which indicate that the crystalline weight fraction within the rigid polyester domains in linear condensation (polyether–polyester) block copolymers increases as the overall polyester weight fraction increases. Taken together, the experimental evidence from n.m.r. and calorimetry suggests, in a nonrigorous manner, that the broad range of molecular motions in the polyester domains might be characterized by an average correlation frequency faster than twice 50 kHz (at the $T_{1\rho}$ minimum). Solid-state deuterium n.m.r. studies[53] reveal that the phenyl rings in crystalline regions of poly(butylene terephthalate) are essentially static, on the n.m.r. timescale. Furthermore, $T_{1\rho}(^{13}C)$ data for the methylene carbons in the polyester segments of several Hytrel copolymers indicate that spin–lattice relaxation is the consequence of thermal motions whose frequencies are, on average, slower than the r.f. field strength in the mid-kilohertz regime[55]. These results are not in agreement with the trends observed for $T_{1\rho}(^1H)$ vs. Hytrel polyester weight fraction data in the present study. On the other hand, Jelinski and coworkers also report that (i) phenyl ring flips in the amorphous regions of PBT have a correlation time of 1.8×10^{-6} s at 70°C[53] (activated rate process with a barrier of 5.9 kcal mol^{-1}, (ii) the methylene carbons in the crystalline regions of PBT undergo conformational isomerizations characterized by a correlation time of 7×10^{-6} s at 20°C[56], and (iii) solid-state ^{13}C T_1 values for the Hytrel copolymers suggest that the methylene carbons in the polyester segments have a significant spectral density of micro-Brownian motions in the megahertz frequency regime[55]. These results are consistent with the data presented here for the polyester segments of the Hytrel copolymers. The role of spin diffusion within the polyester proton nuclear reservoir might be responsible for the fact that our $T_{1\rho}(^1H)$ data reflect motions on the high-frequency side of $T_{1\rho}(^1H)$ minimum.

As mentioned above, the polyether-rich domains in the Hytrel copolymers are highly mobile and void of crystallinity. The data in *Table 3* indicate that $T_{1\rho}(^1H)$ is not completely averaged within the polyether segments. In all cases studied, proton spin–lattice relaxation is slower when measured at the interior methylene carbons relative to the exterior oxygen-linked carbons. This suggests that intradomain dipolar communication between the polyether protons is weak[51], at least for the copolymers containing 33, 34 and 50 wt% polyester. In fact, for the copolymer samples (33 and 34 wt% polyester) in which $T_{1\rho}(^1H)$ measured at the interior methylene carbons exceeds 100 ms, it is highly probable that some of the assumptions used to arrive at equation (1) are actually violated. Hence, an accurate value of $T_{1\rho}(^1H)$ is not reported here. In these situations, the following condition

$$T_{1\rho}^{*}(^{13}C) \approx T_{1\rho}(^1H) \qquad (2)$$

is probably a more realistic representation of the time constants that characterize relaxation between the appropriate nuclear reservoir and the lattice. Here, $T_{1\rho}^{*}(^{13}C)$ is the carbon rotating-frame relaxation time in the presence of high-power ^1H decoupling. This suggests that there are at least two competing pathways by which carbon magnetization can be drained at long contact times during a cross-polarization experiment.

The trend of the data in *Table 3* indicates a decrease in the polyether $T_{1\rho}(^1H)$ time constants as the overall polyester content of the copolymer is increased. Since molecular motion of the soft-segment polyether carbons is known to be on the fast correlation-time side of the $T_{1\rho}(^1H)$ minimum[51], our data suggest that the large-scale mobility of the polyether chains becomes more restricted with increasing polyester content in the copolymer. This tentative conclusion is supported by the ^{13}C relaxation time studies of Jelinski and coworkers[55]. Furthermore, our conclusion is borne out by the increase in soft-segment T_g with increasing polyester content via calorimetric observations[18]. The data in *Table 3* also suggest that

Table 3 Cross-polarization contact-time parameters at various carbon locations in the Hytrel block copolymers

	$T_{1\rho}(^1H)$ (ms)			
PBT (wt%)	33	34	50	68
PTMO M_n	10^3	2×10^3	10^3	10^3
Polyester (PBT)				
carbonyl	6.5	5.2	3.4 (24.1)[b]	3.3 (16.9)
aromatics	6.9	4.8	3.7	3.3 (22.5)
	7.9	5.1	3.7 (55.3)	3.4 (18.2)
OCH_2	6.3	5.2	3.3	3.5
Polyether (PTMO)				
OCH_2	29.8	>40[a]	12.2 (13.1)	6.7 (6.7)
interior methylenes	>100[a]	>100[a]	21.7 (23.1)	7.7 (10.3)

[a] The CP contact-time data are not described accurately by equation (1)
[b] The values in parenthesis are time constants for copolymers with completely deuterated polyester segments

at 68 wt% polyester, there is enough intersegment mixing in the mobile domains to strengthen proton dipolar communication to the extent that the $T_{1\rho}(^1H)$ time constants for the polyether carbons are essentially averaged by spin diffusion. Hence, the n.m.r. results favour a morphological description of the Hytrel copolymers in which a substantial fraction of uncrystallized polyester segments are well mixed in the polyether-rich amorphous domains.

SUMMARY

High-resolution ^{13}C n.m.r. spectroscopy has been used to investigate mixing at the molecular level in (i) a blend of poly(methyl methacrylate) with dinitrobiphenyl and (ii) a series of well characterized polyether–polyester block copolymers. In the polymer–diluent blend, one observes intermolecular cross-polarization transfer from ^1H nuclei in the diluent to ^{13}C nuclei in the perdeuterated polymer. This is evidence for intimate mixing on a molecule-for-molecule basis. In the short-segmented block copolymers (Hytrel copolymers), one observes the transfer of magnetization from polyether protons to polyester carbons. However, it was not possible to distinguish between intersegment and intermolecular cross-polarization mechanisms in the Hytrel copolymers having completely deuterated polyester segments. Nevertheless, the n.m.r. results argue in favour of a morphological description of Hytrel that places a substantial fraction of uncrystallized polyester segments in the well mixed polyether-rich amorphous regions. These conclusions are supported by results from thermal analysis.

ACKNOWLEDGEMENTS

The author is grateful to the Petroleum Research Fund administered by the American Chemical Society for partial support of this work through Grant No. 16208-G7. Funds were also obtained from the Colorado State University Research Foundation through its Resources for Scholarly Programs and an ASEE Summer Faculty Fellowship at the Solar Energy Research Institute, Golden, Colorado. Special thanks are due to Professor Stuart L. Cooper, University of Wisconsin–Madison, for providing duPont's Hytrel copolymers. F. C. Schilling and H. Schonhorn of AT&T Bell Laboratories were kind enough to characterize the percentage deuteration of the d_8-PMMA used in this study via n.m.r. and *FT*i.r. spectroscopies. The solid-state n.m.r. work described herein was performed at the Regional NMR Center, Colorado State University, funded by NSF under grant no. CHE-820881. Finally, Ms Sharon Patterson deserves warm thanks for typing the manuscript.

REFERENCES

1 Olabisi, O., Robeson, L. M. and Shaw, M. T. 'Polymer–Polymer Miscibility', Academic Press, New York, 1979
2 'Polymer Blends and Composites in Multiphase Systems', (Ed. C. D. Han), ACS Adv. Chem. Series **206**, 1984
3 'Multiphase Polymers', (Eds. S. L. Cooper and G. M. Estes), ACS Adv. Chem. Series **176**, 1979
4 'Polymer Blends', (Eds. D. R. Paul and S. Newman), Academic Press, New York, 1978
5 Manson, J. A. and Sperling, L. M. 'Polymer Blends and Composites', Plenum, New York, 1976
6 'Copolymers, Polyblends and Composites', (Ed. N. A. J. Platzer), ACS Adv. Chem. Series **142**, 1975
7 Patterson, D. *Polym. Eng. Sci.* 1982, **22**, 64
8 'Plasticization and Plasticizer Processes', (Ed. N. A. J. Platzer), ACS Adv. Chem. Series **48**, 1965
9 Jackson, W. J. and Caldwell, J. R. *J. Appl. Polym. Sci.* 1967, **11**, 211, 227
10 Belfiore, L. A. and Cooper, S. L. *J. Polym. Sci., Polym. Phys. Edn.* 1983, **21**, 2135
11 Sanchez, I. C. *Polym. Eng. Sci.* 1984, **24**, 79
12 Vallance, M. A. and Cooper, S. L. *Macromolecules* 1984, **17**, 1208
13 Helfand, E. and Wasserman, Z. R. *Macromolecules* 1976, **9**, 879
14 Gordon, M. and Taylor, J. S. *J. Appl. Chem.* 1952, **2**, 493
15 Gordon, M. and Taylor, J. S. *Rubber Chem. Technol.* 1953, **26**, 323
16 Wood, L. A. *J. Polym. Sci.* 1958, **28**, 319
17 Petrie, S. E. B., Moore, R. S. and Flick, J. R. *J. Appl. Phys.* 1972, **43**, 4318
18 Lilaonitkul, A. Ph.D. Thesis, University of Wisconsin–Madison, 1978
19 Belfiore, L. A. and Cooper, S. L. *Polymer* 1984, **25**, 645
20 Hartmann, S. R. and Hahn, E. L. *Phys. Rev.* 1962, **128**, 2042
21 Pines, A., Gibby, M. G. and Waugh, J. S. *J. Chem. Phys.* 1973, **59**, 569
22 Schaefer, J., Stejskal, E. O., Sefcik, M. D. and McKay, R. A. *Macromolecules* 1981, **14**, 188, 275
23 Mehring, M. 'NMR—Basic Principles and Progress', (Eds. E. Fluck, P. Diehl and R. Kosfeld), Springer-Verlag, Berlin/Heidelberg/New York, 1976, Vol. 11, Chap. 4
24 Schaefer, J., Stejskal, E. O. and Buchdahl, R. *Macromolecules* 1977, **10**, 384
25 Stejskal, E. O., Schaefer, J. and Steger, T. R. *Symp. Faraday Soc.* 1979, **13**, 56
26 Wind, R. A., Anthonio, F. E., Duijvestijn, M. J., Smidt, J., Trommel, J. and de Vette, G. M. C. *J. Magn. Reson.* 1983, **52**, 424
27 Stejskal, E. O. and Schaefer, J. *J. Magn. Reson.* 1975, **18**, 560
28 Robertson, R. E. *J. Polym. Sci., Polym. Lett. Edn.* 1979, **17**, 213
29 Bovey, F. A. 'High Resolution NMR of Macromolecules', Academic Press, New York, 1972, Chap. 3
30 Biros, J., Larina, T., Trekoval, J. and Pouchly, J. *Colloid Polym. Sci.* 1982, **260**, 27
31 O'Reilly, J. M. '28th Macro. Symp. Proc.; IUPAC', Amherst, Mass., July 1982, p. 527
32 Belfiore, L. A., Henrichs, P. M., Massa, D. J., Zumbulyadis, N., Rothwell, W. P. and Cooper, S. L. *Macromolecules* 1983, **16**, 1744
33 McArthur, D. A., Hahn, E. L. and Walstadt, R. E. *Phys. Rev.* 1969, **188**, 609
34 Abragam, A. 'The Principles of Nuclear Magnetism', Oxford University Press, London/New York, 1961, Chap. 8
35 McCall, D. W. *Acc. Chem. Res.* 1971, **4**, 223
36 Jelinski, L. W., Dumais, J. J. and Engel, A. K. *Macromolecules* 1983, **16**, 403
37 Imada, K., Miyakawa, T., Chatani, Y., Tadokoro, H. and Murahashi, S. *Makromol. Chem.* 1965, **83**, 113
38 Belfiore, L. A., unpublished results
39 Yoshida, S., Suga, H. and Seki, S. *Polym. J.* 1973, **5**, 25
40 Earl, W. M. and Vander Hart, D. L. *Macromolecules* 1979, **12**, 762
41 Cholli, A. L., Ritchey, W. M. and Koenig, J. L. *Spectrosc. Lett.* 1983, **16**, 21
42 Fleming, W. W., Fyfe, C. A., Kendrick, R. D., Lyerla, J. R., Vanni, H. and Yannoni, C. S. 'Polymer Characterization by ESR and NMR', (Eds. F. A. Bovey and A. E. Woodward), ACS Symp. Series 1980, **142**, 193
43 Schilling, F. C., Bovey, F. A., Tonelli, A. E., Tseng, S. and Woodward, A. E. *Macromolecules* 1984, **17**, 728
44 Cholli, A. L. Ph.D. Thesis, Case Western Reserve University, 1983
45 Aujla, R. S., Harris, R. K., Packer, K. J., Parameswaran, M., Say, B. J., Bunn, A. and Cudby, M. E. A. *Polym. Bull.* 1982, **8**, 253
46 Vander Hart, D. L. and Atalla, R. H. *Macromolecules* 1984, **17**, 1465
47 Saito, H., Tabeta, R., Shoji, A., Ozaki, T. and Ando, I. *Macromolecules* 1983, **16**, 1050
48 Asakura, T., Suzuki, H. and Watanabe, Y. *Macromolecules* 1983, **16**, 1024
49 Tonelli, A. E. *Macromolecules* 1979, **12**, 252; 1983, **16**, 604
50 Tonelli, A. E. and Schilling, F. C. *Acc. Chem. Res.* 1981, **14**, 233
51 Jelinski, L. W., Schilling, F. C. and Bovey, F. A. *Macromolecules* 1980, **14**, 581
52 Schilling, F. C., personal communications
53 Cholli, A. L., Dumais, J. J., Engel, A. K. and Jelinski, L. W. *Macromolecules* 1984, **17**, 2399
54 Vallance, M. A., personal communications
55 Jelinski, L. W., Dumais, J. J., Watnick, P. I., Engel, A. K. and Sefcik, M. D. *Macromolecules* 1983, **16**, 409
56 Jelinski, L. W., Dumais, J. J. and Engel, A. K. *Macromolecules* 1983, **16**, 492